



Crack identification method in beam-like structures using changes in experimentally measured frequencies and Particle Swarm Optimization

Samir Khatir^a, Kevin Dekemele^a, Mia Loccufier^a, Tawfiq Khatir^b,
Magd Abdel Wahab^{c,d,e,*}

^a Department of Electrical Energy, Metals, Mechanical Constructions, and Systems, Faculty of Engineering and Architecture, Ghent University, Ghent, Belgium

^b Institute of Science and Technology, University Center Salhi Ahmed Naama, Algeria

^c Division of Computational Mechanics, Ton Duc Thang University, Ho Chi Minh City, Viet Nam

^d Faculty of Civil Engineering, Ton Duc Thang University, Ho Chi Minh City, Viet Nam

^e Soete Laboratory, Faculty of Engineering and Architecture, Ghent University, Technologiepark Zwijnaarde 903, B-9052 Zwijnaarde, Belgium

ARTICLE INFO

Article history:

Received 23 June 2017

Accepted 28 November 2017

Available online 10 January 2018

Keywords:

Crack detection

Vibration analysis

Particle swarm optimization

Finite element method

Experimental modal analysis

ABSTRACT

In this paper, a technique is presented for the detection and localization of an open crack in beam-like structures using experimentally measured natural frequencies and the Particle Swarm Optimization (PSO) method. The technique considers the variation in local flexibility near the crack. The natural frequencies of a cracked beam are determined experimentally and numerically using the Finite Element Method (FEM). The optimization algorithm is programmed in MATLAB. The algorithm is used to estimate the location and severity of a crack by minimizing the differences between measured and calculated frequencies. The method is verified using experimentally measured data on a cantilever steel beam. The Fourier transform is adopted to improve the frequency resolution. The results demonstrate the good accuracy of the proposed technique.

© 2017 Académie des sciences. Published by Elsevier Masson SAS. All rights reserved.

1. Introduction

In order to identify the location and depth of a crack in a beam, various experimental studies have been conducted, and several methods were proposed by many authors in recent years [1–8]. Structural Health Monitoring (SHM) using vibration analysis is based on five levels, which are: 1) detection; 2) localization; 3) classification; 4) assessment, and 5) prediction. Many previous works for most of these levels are available in the literature. Beams are essential parts of a structure in various fields of engineering and are considered in mechanical, civil, as well as aerospace engineering. In the vibration-based SHM, it is very critical to extract modal parameters information based on the structural response measurements. The information of a structure provides accuracy and critical data for determining the health of a structure, for which the vibration-based SHM plays an essential role. Doebling et al. [9] presented a review on crack identification, damage detection,

* Corresponding author.

E-mail addresses: magd.abdelwahab@tdt.edu.vn, magd.abdelwahab@ugent.be (M. Abdel Wahab).

and localization in structures using vibration analysis. The estimation methods were predominately based on the changes in natural frequencies [10–12]. The multiple damage detection in cantilever beam and complex structures using the coordinate modal assurance criterion combined with an optimization technique was presented by Khatir et al. [13]. The crack has been modeled as a spring with bilinear stiffness by Ballo [14]. Different detection procedures for damage identification in rotors using damage parameters such as the crack depth and location were identified in [15,16]. Based on changes in natural frequencies, Messina et al. [17] calculated the Damage Location Assurance Criterion (DLAC) to identify single damage, which was later extended to identify multiple damages [18]. Lee [19] proposed a technique for the identification of cracks in a beam using Boundary Element Method (BEM). The detection of a crack in a beam was designed in such a way that the crack was not modeled as a massless rotational spring, and then the problem was solved based on natural frequencies using BEM. Deokar and Wakchaure [20] performed experimental tests for the purpose of crack detection in beam-like structures using natural frequencies.

The above technique is called the response-based approach since the response data are directly related to damage [3, 21]. This approach is therefore fast and inexpensive. Another method known as the model-based approach [22] has been proposed to detect damage based on updating certain parameters to get perfect agreement between the experimental measured modal parameters and an initial finite element model. For damage detection in a beam using Genetic Algorithm (GA) and vibration data, three objective functions were used by Khatir et al. [23]. Khatir et al. [24] presented a new damage detection and quantification technique based on the changes in vibration parameters using BAT and PSO algorithms to detect single and multiple-damage positions and the rate of damage in structural elements. The simplest method in a Finite Element (FE) model is to use a reduced stiffness to simulate a small crack [25–27]. Cam et al. [28] presented a technique for damage detection, in which the vibrations as result of impact shocks were analyzed. Friswell and Penny [29] have presented different approaches to model cracks, and showed that for SHM using low frequencies produced good results.

This paper is divided into five main sections. After the introduction section, the damage detection algorithm is presented in the second section. Numerical examples of a 1-D cantilever beam and of a 2-D frame structure are illustrated in section 3. In section 4, experimental validation using a laboratory steel beam is presented. Finally, the paper is concluded with some remarks in section 5.

2. PSO algorithm

Khatir et al. [30] presented a new approach for detecting and locating single damage based on the FEM and the Proper Orthogonal Decomposition method with Radial Basis Function (POD-RBF) coupled with Genetic Algorithm (GA) and PSO algorithm. The results of both algorithms showed that PSO could be used to detect damage with height accuracy. The PSO method was based on swarm intelligence and has been used widely in recent years. It was developed based on a variety of versions that could handle the majority of optimization problems [31,32]. In this study, we used PSO for damage detection in 1-D and 2-D structures. The swarm is modeled as a number of individual particles chosen based on the problem description for a global optimum. The particles communicate with their neighbors over the progress made so far and adjust their moving velocity according to the information given. First, a population of candidate solutions is created randomly, each of which is considered to be a particle moving through the multidimensional design space in search of the position of a global optimum. The particle can be characterized by its physical position in the space and its velocity vector, while it has the ability to remember two important pieces of information, namely; a) the best position has passed so far or a personal best (P_best) and b) the best position that any other particle of the swarm has passed so far or a global best (G_best). The acceleration coefficients of PSO, c_1 and c_2 , represent the degrees of confidence in the best solution found by the individual particles. The updated equations for the speed and position of a particle are:

$$\{v^i(t+1)\} = w\{v^i(t)\} + c_1\{r_1\} \times (\{x^{Pb,j}\} - \{x^j(t)\}) + c_2\{r_2\} \times (\{x^{Gb}\} - \{x^j(t)\}) \quad (1)$$

$$\{x^i(t+1)\} = \{x^i(t)\} + v^i(t+1) \quad (2)$$

where w is an inertia weight parameter, $\{x^{Pb,j}\}$ is a vector of the personal best location found by the particle j until current iteration, $\{x^{Gb}\}$ is a vector of the global best location found by the entire swarm up to the current iteration, $\{v^i(t)\}$ is the velocity vector of particle j at time t , $\{x^j(t)\}$ is the position vector of particle j at time t , and r_1, r_2 are vectors containing random numbers with uniform distribution in the interval $[0, 1]$.

The fitness of each particle shows the quality of each solution and is evaluated by an objective function. In every iteration, the speed of the particle is updated in a stochastic way. In this paper, we use PSO as an inverse problem for detecting and locating damage using measured and calculated natural frequencies. The objective function (OF) is presented in the following form:

$$OF = \sum_i^n ((\omega_i^f - \omega_i^c)^2 / (\omega_i^c)^2) \quad (3)$$

where, n is the number of modes, ω_i^f are the frequencies calculated by PSO-FEM, and ω_i^c are the experimentally measured frequencies.

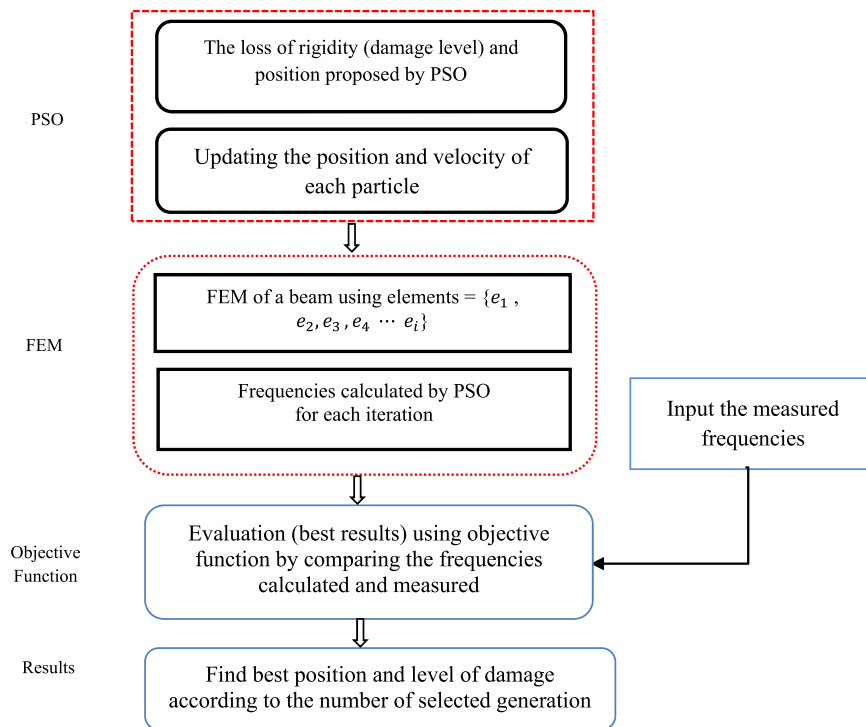


Fig. 1. Methodological approach for damage detection using PSO-FEM.

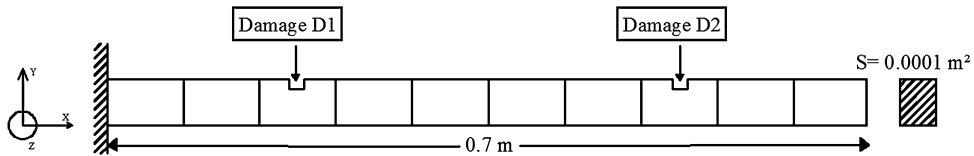


Fig. 2. Beam discretized into 10 elements.

The PSO approach is used with population size of 200 individuals and maximum generation number of 100. The principle of the methodological approach can be more easily seen through the flowchart given in Fig. 1.

3. Numerical examples

In this section, the results of two configurations, a cantilever beam and a 2-D frame structure, are presented using simulated data. The number of iterations for the cantilever beam was set between 10 and 25, while for the 2-D frame structure the number of iterations was set between 30 and 40. The fitness tolerance was introduced to be equal to zero. This proposed method was implemented in MATLAB, on a PC with an Intel I5 Processor 5.0 GHz and 8 GB RAM.

3.1. A cantilever beam

For this first example, the model under study is a fixed-free beam divided into 10 elements and 11 nodes, with two damage scenarios, D1 and D2, as it can be seen in Fig. 2. Only two degrees of freedom, a vertical translation y and a rotation θ_z are allowed. The length of the beam is 0.7 m, the cross-section area is 0.0001 m^2 , the Young modulus is 200 GPa, and the density is 7800 kg/m^3 .

The results of a single damage with 30% loss of rigidity at element 3 (D1) are shown in Fig. 3, and in Fig. 4 for a single damage at element 8 (D2). The results show that for both damage scenarios, positions and levels were determined with high precision after only 10 iterations.

3.2. A two-dimensional frame

A 20-bar complex 2-D frame structure, shown in Fig. 5, is studied as a second example. The length of each horizontal bar is 1 m, and the length of the vertical bar is 0.8 m. The cross-section area of each bar is 0.006 m^2 , the Young modulus

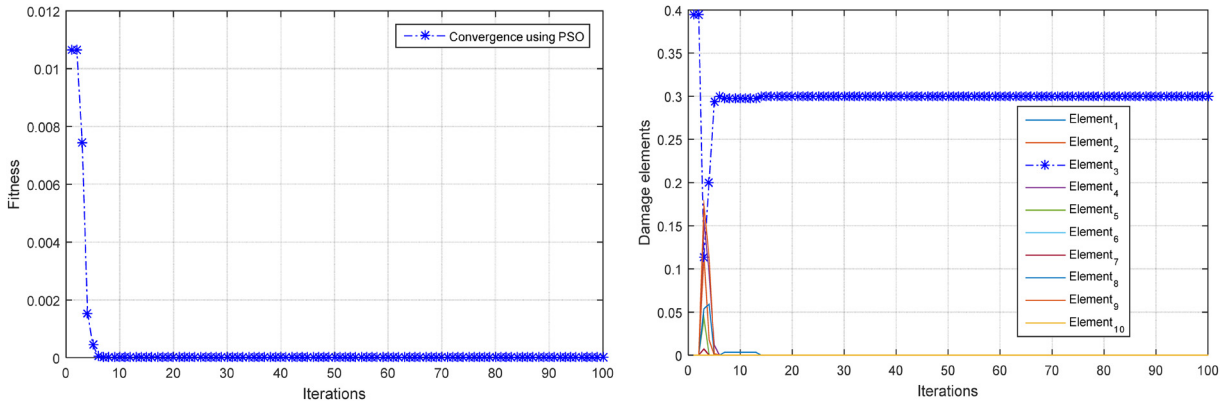


Fig. 3. Fitness and damage elements for D1 with 30% damage level.

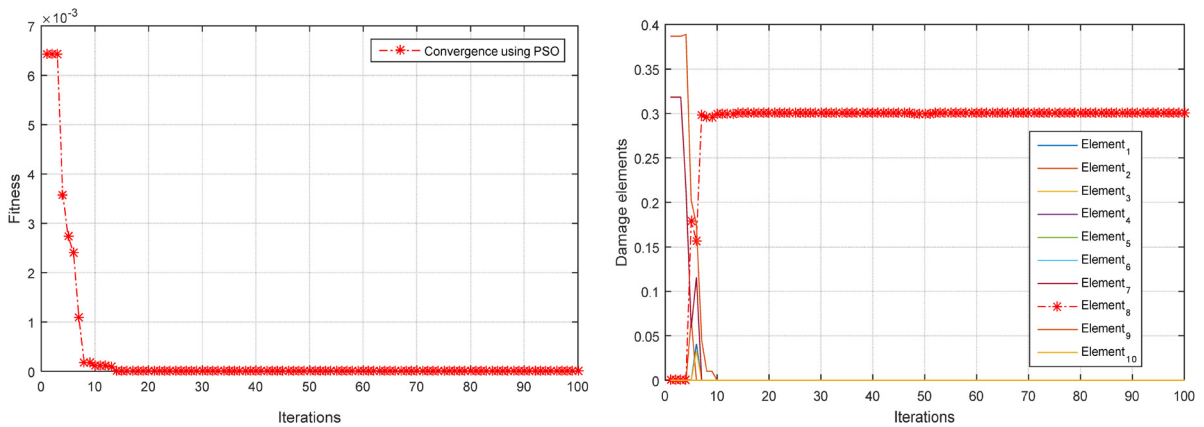


Fig. 4. Fitness and damage in elements for D2 with 30% damage level.

is 200 GPa, and the density ρ is 7800 kg/m³. The total numbers of elements and nodes are 20 and 15, respectively, and two damage scenarios D3 and D4 are considered as shown in Fig. 5. The results of the 2-D frame structure for damage with 30% loss of rigidity at element 5 (D3) are shown in Fig. 6, while the results for damage at element 19 (D4) are shown in Fig. 7. These results demonstrate that this approach can detect the damage positions and severity accurately for a complex structure after 30 iterations.

4. Experimental validation

4.1. Experimental set-up

To verify the accuracy of our approach for crack identification in beam-like structures, an experimental setup was designed using a steel beam (Fig. 8). The dimensions and material properties of the beam are given in Table 1. A Bruel and Kjaer type 8206–001 impact hammer, a Bruel and Kjaer DeltaTron™ type 4507 accelerometer and a National Instruments NI 9234 analog-to-digital converter were used. The transversal accelerations at different locations on the beam, caused by the impact hammer at another location, were measured.

To find the eigenfrequencies experimentally, spectral analysis is performed on the measured input and output. The input, the force of a hammer strike at a specific location, should have a sufficiently broad bandwidth to include all required modes. If this is the case, the output, the transversal acceleration at different locations, will contain many modes. For the input, the discrete Fourier Transform (DFT) is performed to analyze its bandwidth. For the output, the Frequency Response Function (FRF) at the measured positions caused by an excitation at the location of the strike, is used to determine the eigenfrequencies. The FRF is a relative measure, expressed in per applied force at a specific frequency, and is more useful than the DFT of the output as not all frequencies are excited with the same magnitude.

The FRF is estimated with the so-called H1 estimator, see Fig. 9. Here, the measured output $y(t)$ is assumed to be:

$$y(t) = u(t) + n(t) = h(t) * x(t) + n(t) \tag{4}$$

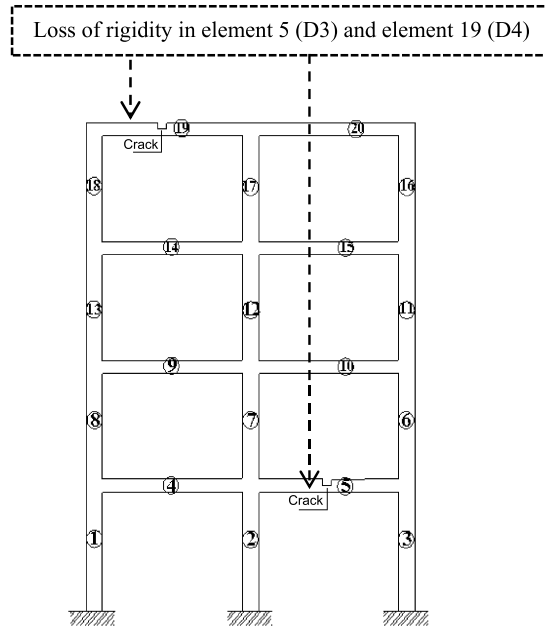


Fig. 5. Two-dimensional frame discretized in 20 elements.

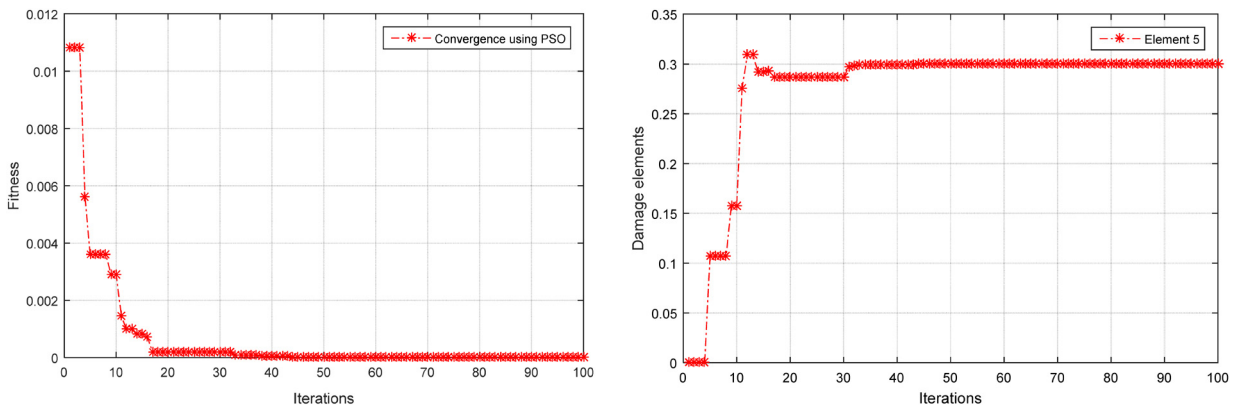


Fig. 6. Fitness and damage in elements for D3 with 30% damage level.

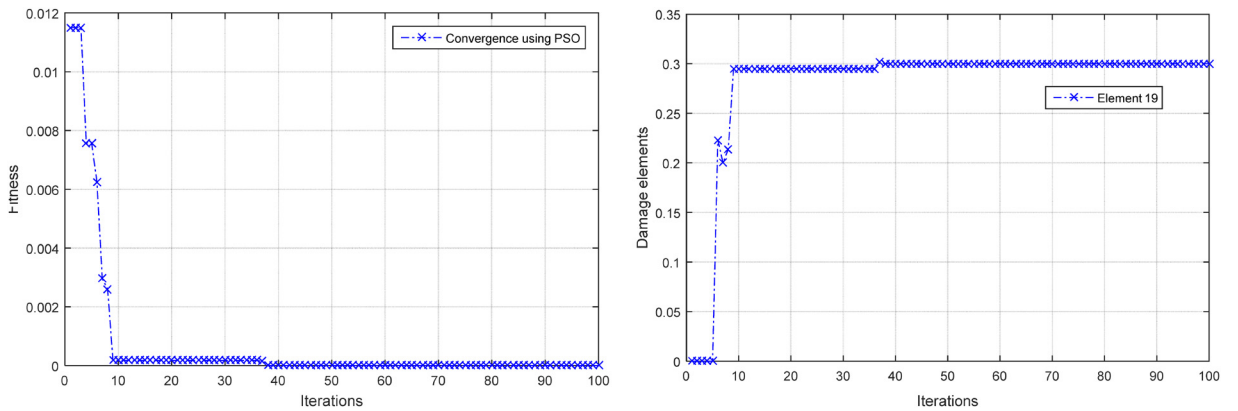


Fig. 7. Fitness and damage in elements for D4 with 30% damage level.



Fig. 8. Experimental set-up.

Table 1
Dimensions and material properties.

Properties	Mean value
Length (m)	0.75
Width (m)	0.025
Thickness (m)	0.006
Young modulus (GPa)	200
Density (kg/m ³)	7800
Poisson's ratio	0.3

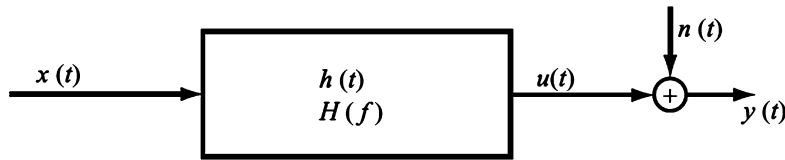


Fig. 9. H1 linear system [33].

where $x(t)$ is the input, $h(t)$ is the impulse response function, $n(t)$ is the white uncorrelated noise and $*$ is the convolution operator. The following relation between the (cross) power density spectra exists:

$$S_{yx} = g_{kl}(i\omega)S_{xx} + S_{nx} \tag{5}$$

where S_{xx} is the power spectral density of the input (= the load at element l), S_{yx} is the cross-power spectral density of the input and the output (= response at element k), and $g_{kl}(i\omega)$ is the FRF at input k caused by the force at l , which is the FT of the impulse response $h(t)$. The cross-power spectral density of the input and the noise S_{nx} is zero as $n(t)$ is uncorrelated noise. Equation (5) is then simplified as:

$$S_{yx} = g_{kl}(i\omega)S_{xx} \tag{6}$$

from which the FRF $g_{kl}(i\omega)$ is estimated.

4.2. Intact beam

A strike of an impact hammer approximates an impulse, which theoretically has a FT of 1 for all frequencies. Fig. 10 plots the time and the DFT of an impact test on the position 50 cm for an undamaged beam.

In the time domain, the impact approximates an impulse and in the frequency domain, it has a large bandwidth. Equation (4) is applied on the applied strike at 50 cm and on the measured acceleration at 70 cm, with the estimate FRF as shown in Fig. 11. Note that only the first four modes are considered.

A FE model for this cantilever beam was constructed using Euler–Bernoulli beam elements as mentioned earlier. The boundary conditions of the beam are free–free, as in the experimental setup the beam was suspended using a very flexible spring. The optimization problem using PSO is solved as described in section 2. The algorithm is firstly applied to the intact beam in order to achieve perfect match with the experimentally measured natural frequencies. The updated parameter in this case was the global Young’s modulus of the beam, which was found to be 2.0786×10^{11} . The converged natural frequencies are listed in Table 2 and compared to the experimentally measured ones. Excellent match can be seen.

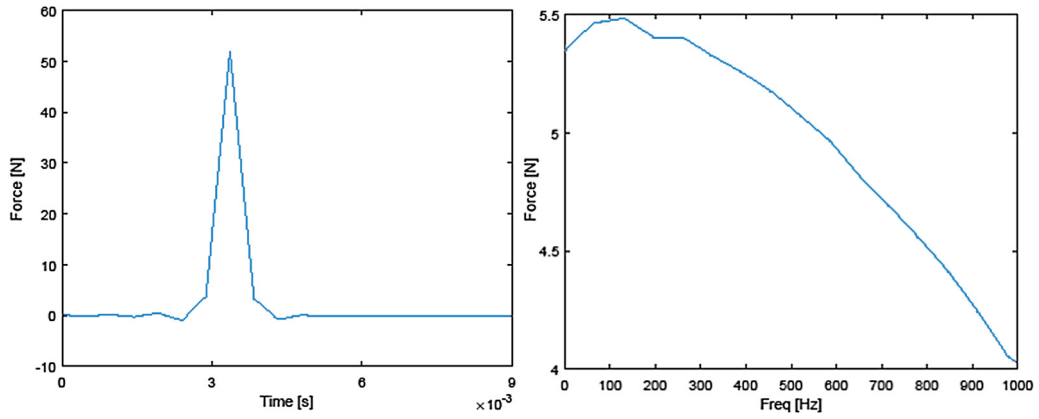


Fig. 10. Input on 50 cm, left time, right DFT.

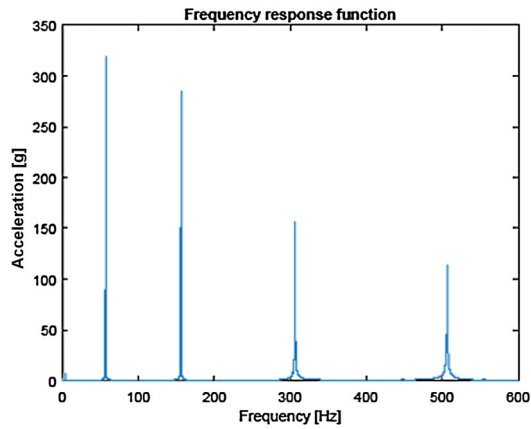


Fig. 11. Frequency response function at 70 cm by a load at 37.5 cm for an undamaged beam.

Table 2
Numerical and experimental natural frequencies of undamaged beam.

Modes	FEM	Experimental	PSO-FEM
1	55.51	56.75	56.75
2	153.02	156.39	156.43
3	300.07	306.19	306.75
4	496.51	506.15	507.56

4.3. Damaged beam

The damaged beam considered herein has a crack at a position of 375 mm with a depth of 1 mm (case 1) and a depth of 3 mm (case 2). The crack is generated using a thin saw cut to a thickness of 0.5 mm as shown in Fig. 12. The FRF of the damaged beam (case 1) is shown on the left-hand side of Fig. 13. If zoomed in, only the third eigenfrequency seems to have shifted significantly (right-hand side in Fig. 13). The FRF of the damaged beam (case 2) is shown in Fig. 14. Herein, a clearer shift in the third mode is seen, as well as a small shift in the first mode.

4.4. Modeling of damage

In the FE model of the laboratory beam, the crack is simulated by calculating a stiffness reduction exponential function, $EI(x)$, for a rectangular beam, which represents the variation in stiffness, given by [34]:

$$EI(x) = \frac{EI}{1 + Ce^{((-2\alpha|X-X_c|)/d)}} \tag{7}$$

where $C = (I_0 - I_{c_j})/I_{c_j}$ for $I_0 = wd^3/12$ and $I_c = w(d - d_c)^3/12$.



Fig. 12. Cracked beam using a saw cut.

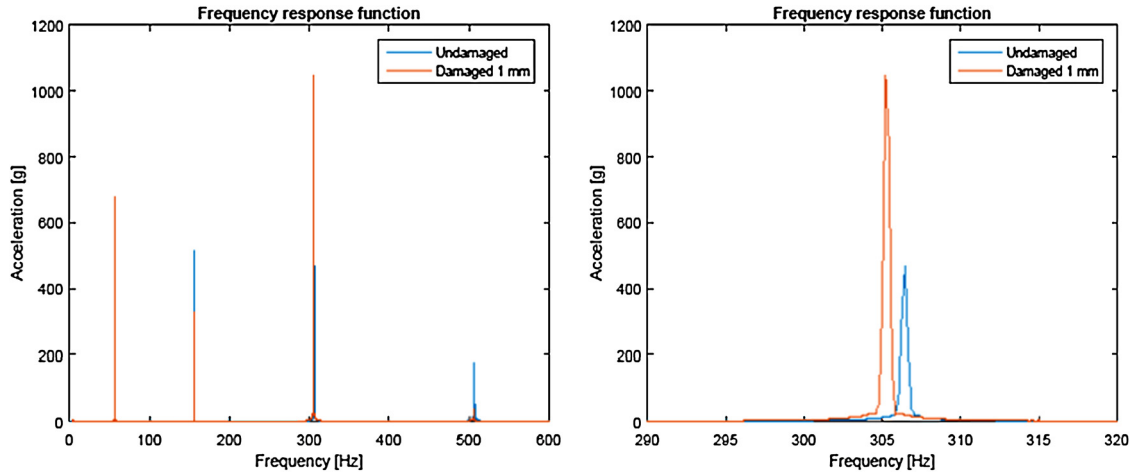


Fig. 13. FRF of the damaged beam with 1-mm crack depth (left), zoomed in (right).

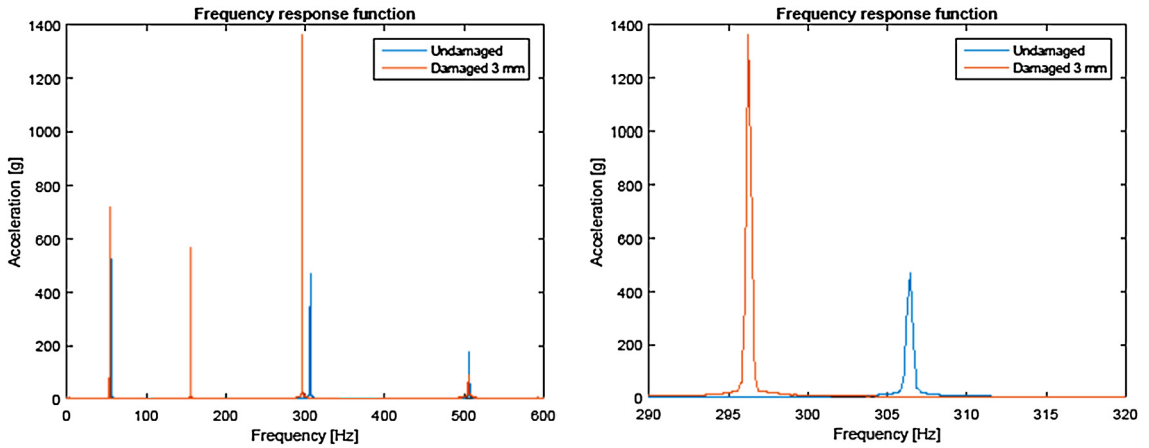


Fig. 14. FRF of damaged beam with 3-mm crack depth (left), zoomed in (right).

As shown in Fig. 15, w and d are the width and the depth of the beam, respectively, d_c is the crack depth, X is any position along the beam, X_c is the position of a crack and α is a constant, which is estimated from the experiments to be 0.667 [19]. Equation (7) is integrated within the approach presented in Fig. 1, section 2.

4.5. Validation results

In the first validation example, case 1 is considered, i.e. crack depth is 1 mm at a position of 0.375 m. The convergence of the position and the depth of the crack is shown in Fig. 16, and the convergence of the fitness is shown in Fig. 17. From the results, it can be seen that, after 10 iterations, both depth and position are converged to the experimental values and the

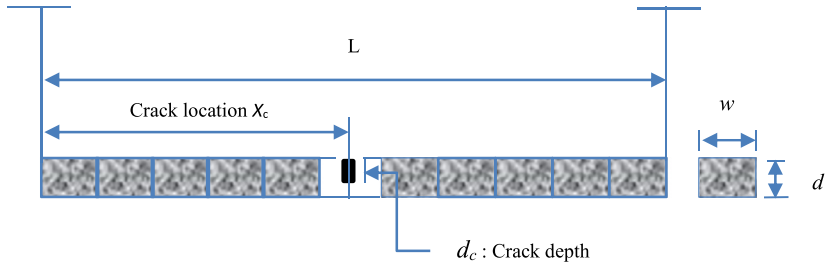


Fig. 15. Simple crack model of a beam.

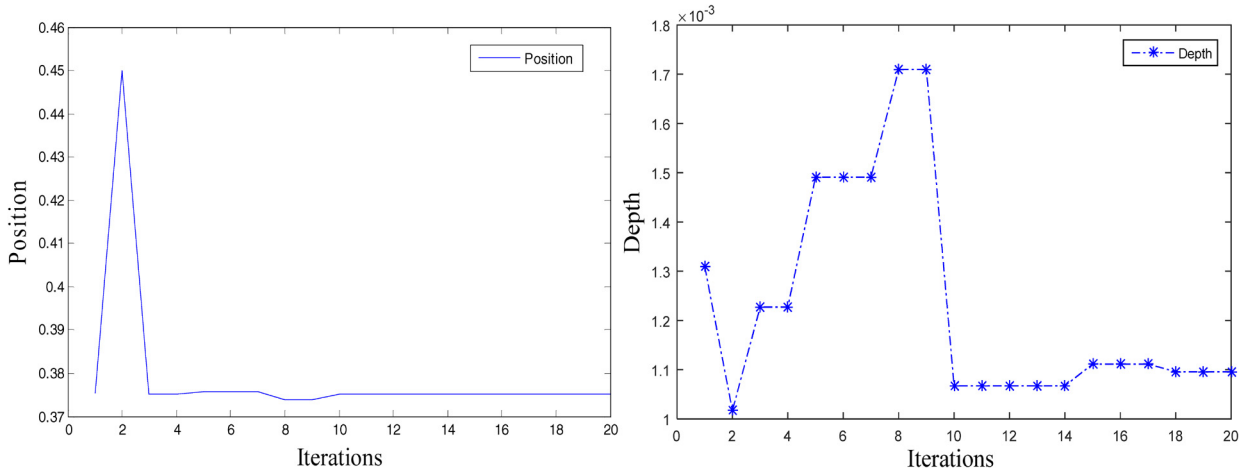


Fig. 16. Convergence of position (right) and depth (left), for a crack depth of 1 mm at a position of 0.375 m.

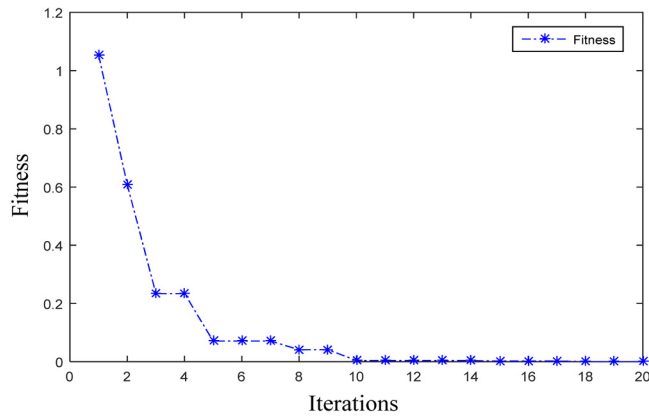


Fig. 17. Convergence of fitness for a crack depth 1 mm at a position of 0.375 m.

Table 3
Natural frequencies (Hz) of a damaged beam having a crack depth of 1 mm at a position of 0.375 m.

Modes	Experimental	PSO-FEM
1	56.3835	56.3097
2	156.3035	156.2323
3	305.4699	305.4152
4	506.0238	506.1066

fitness is converged to zero. The converged natural frequencies using PSO are compared with the experimentally measured ones in Table 3, from which excellent match can be seen.

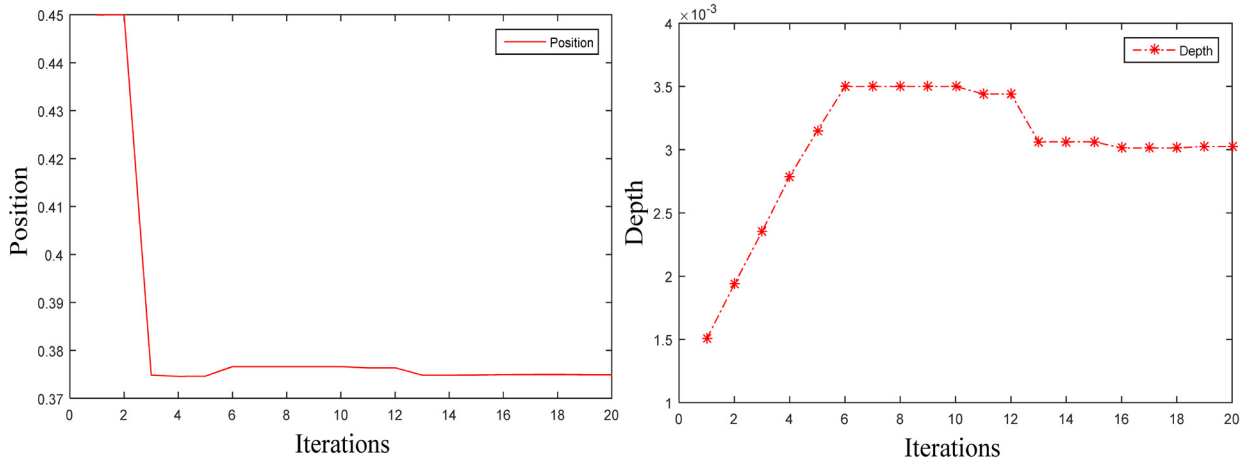


Fig. 18. Convergence of position (right) and depth (left), for a crack depth 3 mm at a position of 0.375 mm.

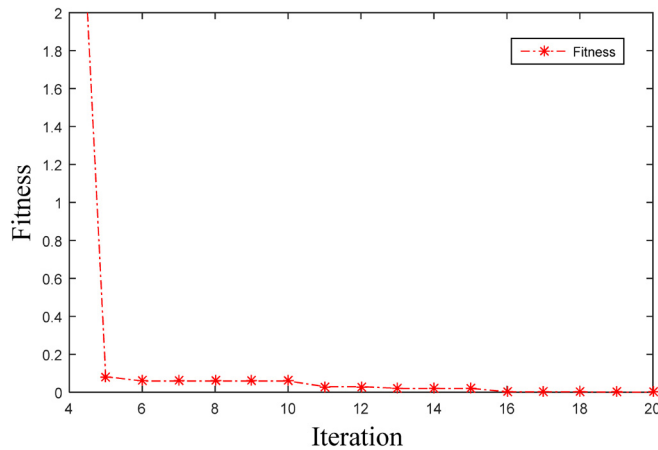


Fig. 19. Convergence of fitness for a crack depth 3 mm at a position of 0.375 m.

Table 4

Natural frequencies (Hz) of a damaged beam having a crack depth of 3 mm at a position of 375 mm.

Modes	Experimental	PSO-FEM
1	54.3088	54.1621
2	156.0788	156.3835
3	296.3372	295.9844
4	505.5442	505.7671

In the second validation example, case 2, the crack depth is increased to 3 mm at the same position of 0.375 m. For this case, the convergence of the position and depth of the crack is shown in Fig. 18 and that of the fitness is illustrated in Fig. 19. After four iterations, both depth and position are converged to the experimental values and the fitness is converged to zero. Comparing these results to those obtained for case 1, it can be concluded that the convergence rate is faster for larger crack depths. This is a logic conclusion as the larger the crack depth the easier to detect using modal data. The converged natural frequencies using PSO are compared with the experimentally measured ones in Table 4 for the case of a crack depth of 3 mm. Again, excellent match can be seen.

As a general conclusion, from the results, it can be seen that the performance of our approach, when a single crack is present, is very good. The depth and location of the crack are very accurately estimated using the measured data of the free-free steel beam.

5. Conclusion

In this paper, a non-destructive method for the estimation of both the location and the depth of a crack in beam-like structures, based on an inverse vibration problem, has been presented. The approach was based on PSO-FEM and experimentally measured modal data for damaged and undamaged beams. The change in the natural frequencies of the structure due to the presence of a crack was used as an objective function. A numerical study using simulated data of two examples, namely a cantilever beam and a 2-D frame structure, were presented. Furthermore, the proposed approach was validated using vibration experiments on a free-free laboratory beam. It has also been observed from our results that the estimation of the crack position and depth was very accurate.

References

- [1] G.R. Gillich, et al., Localization of transversal cracks in sandwich beams and evaluation of their severity, *Shock Vib.* 2014 (2014) 607125, <https://doi.org/10.1155/2014/607125>, 10 pages.
- [2] S. Khatir, et al., Multiple damage detection in composite beams using particle swarm optimization and genetic algorithm, *Mechanika* 23 (4) (2017) 514–521.
- [3] Y.-L. Zhou, et al., Output-based structural damage detection by using correlation analysis together with transmissibility, *Materials* 10 (8) (2017) 866.
- [4] Y.-L. Zhou, M. Abdel Wahab, Cosine based and extended transmissibility damage indicators for structural damage detection, *Eng. Struct.* 141 (2017) 175–183.
- [5] Y.-L. Zhou, et al., Structural damage detection using transmissibility together with hierarchical clustering analysis and similarity measure, *Struct. Health Monit.* 2016 (2016), <https://doi.org/10.1177/1475921716680849>.
- [6] G.-R. Gillich, et al., Free vibration of a perfectly clamped-free beam with stepwise eccentric distributed masses, *Shock Vib.* 2016 (2016) 2086274, <https://doi.org/10.1155/2016/2086274>, 10 pages.
- [7] Y.-L. Zhou, N. Maia, M. Abdel Wahab, Damage detection using transmissibility compressed by principal component analysis enhanced with distance measure, *J. Vib. Control* 2016 (2016), <https://doi.org/10.1177/1077546316674544>.
- [8] Y.-L. Zhou, M. Abdel Wahab, Rapid early damage detection using transmissibility with distance measure analysis under unknown excitation in long-term health monitoring, *J. Vibroeng.* 18 (7) (2016) 4491–4499.
- [9] S.W. Doebling, C.R. Farrar, M.B. Prime, A summary review of vibration-based damage identification methods, *Shock Vib. Dig.* 30 (2) (1998) 91–105.
- [10] P. Cawley, R. Adams, The location of defects in structures from measurements of natural frequencies, *J. Strain Anal. Eng. Des.* 14 (2) (1979) 49–57.
- [11] M. Friswell, J. Penny, D. Wilson, Using vibration data and statistical measures to locate damage in structures, *Int. J. Anal. Exp. Modal Anal.* 9 (4) (1994) 239–254.
- [12] J. Penny, D. Wilson, M. Friswell, Damage location in structures using vibration data, in: *Proceedings of the 11th Modal Analysis Conference*, Kissimmee, FL, USA, 1993, pp. 254–260.
- [13] A. Khatir, et al., Multiple damage detection and localization in beam-like and complex structures using co-ordinate modal assurance criterion combined with firefly and genetic algorithms, *J. Vibroeng.* 18 (8) (2016), <https://doi.org/10.21595/jve.2016.17026>.
- [14] I. Ballo, Non-linear effects of vibration of a continuous transverse cracked slender shaft, *J. Sound Vib.* 217 (2) (1998) 321–333.
- [15] F. Ismail, A. Ibrahim, H. Martin, Identification of fatigue cracks from vibration testing, *J. Sound Vib.* 140 (2) (1990) 305–317.
- [16] S. Cheng, et al., Vibrational response of a beam with a breathing crack, *J. Sound Vib.* 225 (1) (1999) 201–208.
- [17] A. Messina, I. Jones, E. Williams, Damage detection and localization using natural frequency changes, in: *Proc. 14th International Modal Analysis Conference*, Dearborn, MI, USA, 1996.
- [18] A. Messina, E. Williams, T. Contursi, Structural damage detection by a sensitivity and statistical-based method, *J. Sound Vib.* 216 (5) (1998) 791–808.
- [19] J. Lee, Identification of a crack in a beam by the boundary element method, *J. Mech. Sci. Technol.* 24 (3) (2010) 801–804.
- [20] A. Deokar, V. Wakchaure, Experimental Investigation of Crack Detection in Cantilever Beam Using Natural Frequency as Basic Criterion, Institute of Technology, Nirma University, Ahmedabad, India, 2011.
- [21] Y.-L. Zhou, M.A. Wahab, Damage detection using vibration data and dynamic transmissibility ensemble with auto-associative neural network, *Mechanika* 23 (5) (2017) 688–695.
- [22] M.A. Wahab, G. De Roeck, Damage detection in bridges using modal curvatures: application to a real damage scenario, *J. Sound Vib.* 226 (2) (1999) 217–235.
- [23] S. Khatir, I. Belaidi, R. Serra, B. Benaissa, A. Ait Saada, Genetic algorithm based objective functions comparative study for damage detection and localization in beam structures, *J. Phys. Conf. Ser.* 628 (2015) 012035.
- [24] S. Khatir, I. Belaidi, R. Serra, M.A. Wahab, T. Khatir, Numerical study for single and multiple damage detection and localization in beam-like structures using BAT algorithm, *J. Vibroeng.* 18 (1) (2016) 202–213.
- [25] A. Pandey, M. Biswas, M. Samman, Damage detection from changes in curvature mode shapes, *J. Sound Vib.* 145 (2) (1991) 321–332.
- [26] C.P. Ratcliffe, Damage detection using a modified Laplacian operator on mode shape data, *J. Sound Vib.* 204 (3) (1997) 505–517.
- [27] A. Behtani, et al., Damage localization and quantification of composite beam structures using residual force and optimization, *J. Vibroeng.* 19 (7) (2017) 4977–4988.
- [28] E. Çam, S. Orhan, M. Lüy, An analysis of cracked beam structure using impact echo method, *NDT Int.* 38 (5) (2005) 368–373.
- [29] M.I. Friswell, J.E. Penny, Crack modeling for structural health monitoring, *Struct. Health Monit.* 1 (2) (2002) 139–148.
- [30] S. Khatir, et al., Damage detection and localization in composite beam structures based on vibration analysis, *Mechanics* 21 (6) (2016) 472–479.
- [31] V. Plevris, A. Batavanis, M. Papadrakakis, Optimum design of steel structures with the Particle Swarm Optimization method based on EC3, in: *Computational Methods in Structural Dynamics and Earthquake Engineering*, 2011.
- [32] Q. Bai, Analysis of particle swarm optimization algorithm, *Comput. Inf. Sci.* 3 (1) (2010) 180.
- [33] A. Brandt, *Noise and Vibration Analysis: Signal Analysis and Experimental Procedures*, John Wiley & Sons, 2011.
- [34] S. Christides, A. Barr, One-dimensional theory of cracked Bernoulli-Euler beams, *Int. J. Mech. Sci.* 26 (11–12) (1984) 639–648.